Osteoarthritis and Cartilage (2009) **17,** 695–704

doi:10.1016/j.joca.2008.11.003

Osteoarthritis and Cartilage

International Cartilage Repair Society

OARSI OSTEOARTHRITIS RESEARCH SOCIETY INTERNATIONAL

A novel *in vivo* murine model of cartilage regeneration. Age and strain-dependent outcome after joint surface injury

N. M. Eltawil†, C. De Bari‡, P. Achan§, C. Pitzalis†[a] and F. Dell'Accio†*[a]

† *William Harvey Research Institute, Barts and the London Queen Mary's School of Medicine and Dentistry, Centre for Experimental Medicine and Rheumatology, London, UK*

‡ *University of Aberdeen, School of Medicine, Department of Medicine and Therapeutics, Aberdeen, UK*

§ *Barts and The Royal London Hospitals, London, UK*

Summary

Objectives: To generate and validate a murine model of joint surface repair following acute mechanical injury.

Methods: Full thickness defects were generated in the patellar groove of C57BL/6 and DBA/1 mice by microsurgery. Control knees were either sham-operated or non-operated. Outcome was evaluated by histological scoring systems. Apoptosis and proliferation were studied using TUNEL and Phospho-Histone H3 staining, respectively. Type II collagen neo-deposition and degradation were evaluated by immunostaining using antibodies to the CPII telopeptide and C1,2C (Col2-3/4Cshort), respectively. Aggrecanases and matrix metalloproteinases (MMPs) activity were assessed by immunostaining for $TEGE^{373}$ and VDIPEN neo-epitopes.

Results: Young 8-week-old DBA/1 mice displayed consistent and superior healing of the articular cartilage defect. Age-matched C57BL/6 mice repaired poorly and developed features of osteoarthritis (OA). Compared to C57BL/6, DBA/1 mice displayed a progressive decline of chondrocyte apoptosis, cell proliferation within the repair tissue, persistent type II collagen neo-deposition, less type II collagen degradation, less aggrecanases and more MMP-induced aggrecan degradation. Eight-month-old DBA/1 mice failed to repair, but, in contrast to age-matched C57BL/6 mice, developed no signs of OA.

Conclusion: We have generated and validated a murine model of cartilage regeneration in which the outcome of joint surface injury is strain and age dependent. This model will allow, for the first time, the dissection of different pathways involved in joint surface regeneration in adult mammals using the powerful technology of mouse genetics.

Key words: Cartilage repair, Joint surface defects, Cartilage regeneration, Animal models, osteoarthritis, Cartilage injury, apoptosis, Metalloproteinases, regenerative medicine.

Introduction

Joint surface defects (JSD) are observed in over 60% of all arthroscopic procedures[1,2] often are symptomatic and disabling[2,3], associated with cartilage loss, progression towards osteoarthritis (OA), and predict prosthetic joint replacement[4,5]. Cartilage breakdown is the invalidating outcome of most rheumatic conditions causing pain and disability for millions of people world-wide. Therefore, joint surface restoration is a major priority in modern medicine. The natural history of JSD, however, varies from spontaneous healing to OA development[6–8], depending on patient-related factors including age, body weight and co morbidity, as well as factors related to the defect including site, size, depth and severity of the injury[7–10]. Structural and functional restoration of joint surface integrity after chondral or osteochondral lesions has been documented in high number of individuals, in an age-dependent fashion[7,11,12]. Additionally, spontaneous repair has been reported in large animal models of full thickness joint surface injury such as rabbits, dogs and horses[13–15]. These data, along with the fact that the joint environment is rich in progenitor/stem cells[13,16,17], suggest the presence of intrinsic repair mechanisms capable of recruiting resident stem cells to the site of damage and controlling their fate decisions and differentiation[18].

Surgical therapeutic approaches such as microfracture, mosaicplasty and autologous chondrocyte implantation (ACI) are currently used to treat symptomatic localized chronic full thickness chondral lesions[3,19,20]. However, none of these procedures is optimal due to issues related to costs, invasiveness, durability of repair tissue, *in vitro* cell manipulations, outcome variability and difficult up scaling[21,22]. A regeneration process that could be initiated and supported using bioactive compounds delivered at the site of injury to trigger/enhance the intrinsic repair capacity of adult joints would be a desirable alternative approach to overcome these problems[21]. Unfortunately, the understanding of the molecular and cellular mechanisms underpinning the regulation of joint surface healing and, consequently, the identification of potential therapeutic targets has been hindered by the unavailability of well characterized small animal models suitable to test the function of individual

[a]These authors share senior authorship.

*Address correspondence and reprint requests to: Francesco Dell'Accio, Centre for Experimental Medicine and Rheumatology, William Harvey Research Institute, Queen Mary's School of Medicine and Dentistry, II Floor, John Vane Building, Charterhouse Square, London EC1M 6BQ, UK. Tel: 44-(0)-20-7882-8204; E-mail: f.dellaccio@qmul.ac.uk

Received 8 May 2008; revision accepted 4 November 2008.

molecules involved in joint surface repair, since all the currently available models exist in large animals[13–15] that are not amenable for genetic manipulation. In this study, we have generated and validated a murine model in which the repair outcome of a well controlled, consistent and reproducible joint surface injury is dependent on the strain and the age of the mice. This work describes a novel joint surface regeneration model in adult animals, in a species that is widely validated as a preclinical model and that is amenable to genetic manipulation, thus allowing functional molecular studies in the process of joint surface healing.

Materials and methods

OPERATIVE PROCEDURE

All procedures were approved by the Local Ethics committee and the UK Home Office.

Male mice were anesthetized using ketamine (40 mg/kg) and xylazine (5 mg/kg). Medial para-patellar arthrotomy was performed under a dissection microscope (Leica), by inserting microsurgical scalpel medially and proximally to the insertion of the patellar tendon on the tibia and extending it proximally until the attachment of the quadriceps muscle. The medial margin of the quadriceps was separated from the muscles of the medial compartment. The joint was extended and the patella was dislocated laterally. The joint was then fully flexed to expose the patellar groove. A longitudinal full thickness injury was made in the patellar groove using a custom made device in which a glass bead was placed approximately 200 μm to the tip of a 26 G needle (Fig. 1A). The tip of the needle was placed anteriorly to the intercondylar notch and gently moved along the entire length of the patellar groove (Fig. 1A). The patellar dislocation was then reduced. The joint capsule and the skin were sutured in separate layers. The contra-lateral knee was either left non-operated or subjected to arthrotomy and patellar dislocation without cartilage injury (sham-operated controls). The number of mice in each age group, at each time point is shown in Table I.

TISSUE PROCESSING AND HISTOLOGY

Knee joints were fixed, decalcified, paraffin embedded and serially sectioned at 5 μm interval. Only sections between planes A and C (Fig. 1B) were used for analysis. Plane A is 100 μm proximal to the intercondylar notch, plane B is 100 μm proximal to plane A and plane C is 100 μm proximal to plane B. Within this interval, the sections intercept the growth plate in four points and this was used as landmark for section level (Fig. 1B). Sections A, B, and C were used for histomorphometry and scoring. The other sections comprised in the A–C interval were used for immunohistochemical staining. Hematoxylin & eosin and safranin-O fast green staining (for highly sulfated, negatively charged glycosaminoglycans) were performed according to standard protocols. Slides were analyzed with an Olympus BX61 microscope and Cell-P software (Olympus UK Ltd, UK).

Table I
The number of mice killed per time point

Strain	Age	No. of animals	Time point
DBA/1	8 Weeks	15	8 Weeks
C57Bl/6	8 Weeks	15	8 Weeks
DBA/1	8 Months	15	8 Weeks
C57Bl/6	8 Months	15	8 Weeks
DBA/1	8 Weeks	5	1 Day
C57Bl/6	8 Weeks	5	1 Day
DBA/1	8 Weeks	5	1 Week
C57Bl/6	8 Weeks	5	1 Week
DBA/1	8 Weeks	5	4 Weeks
C57Bl/6	8 Weeks	5	4 Weeks
Total		90	

HISTOMORPHOMETRY AND SCORING

Histomorphometry and scoring were performed at the levels indicated in Fig. 1B and the values were averaged for each knee. Cartilage thickness, depth, cross-sectional width (CSW) and cross-sectional area (CSA) of the JSD were measured 1 day after joint surface injury. The defect-depth/cartilage thickness ratio and the coefficient of variation were represented as percentage. Joint surface repair was scored as previously described[23,24] and OA was assessed using Modified Mankin score[25,26]. Scoring was performed independently by two observers blinded to the group assignment. All the data are expressed as the mean ± standard error of the mean (S.E.M.).

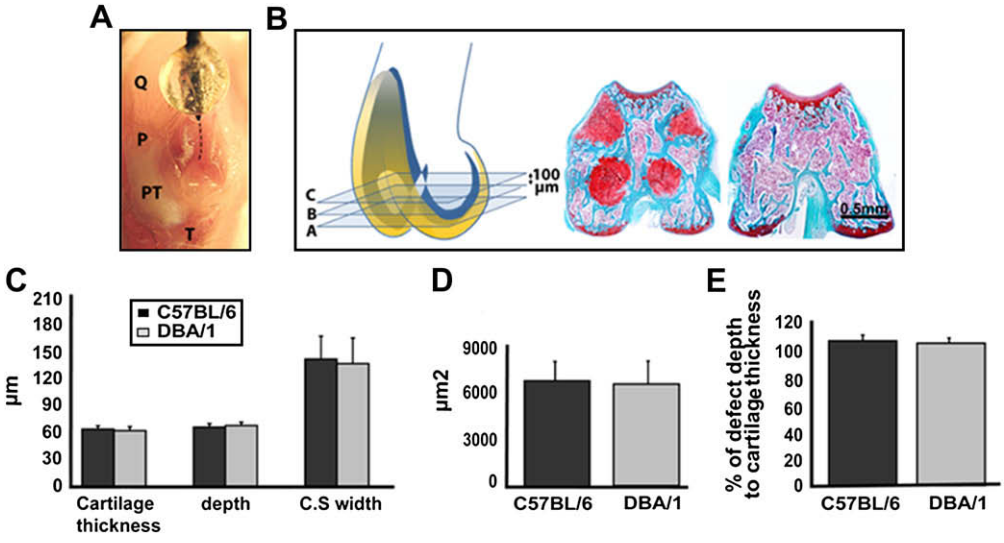

Fig. 1. Consistency and reproducibility of surgically induced full thickness JSD. (A) Cadaveric preparation (right knee joint) to show the generation of a full thickness defect in the patellar groove. The patellar groove is exposed by lateral dislocation of the patella (P). The devise is placed with its tip just anteriorly to the intercondylar notch (lower end of dotted line) and dragged proximally in the centre of the entire length of patellar groove (dotted line). (B) Schematic representation of a mouse knee joint (articular cartilage in yellow and the growth plate in blue). All the sections comprised between A and C intersects the growth plate in 4 points (sections A–C on the left). This landmark is absent in sections outside this interval (section on the right). (C–E), Histomorphometric comparison of cartilage thickness, depth and CSW of the defect (B), CSA (C) and the percentage of defect depth to cartilage thickness (D) in C57BL/6 and DBA/1 mice 1 day after surgery ($n = 5$). All the values are expressed as mean ± standard error of the mean (S.E.M.). P = patella; PT = patellar tendon; Q = quadriceps muscle and T = tibial tuberosity.
[For interpretation of color in this figure legend, the reader is referred to web version of the article.]

APOPTOSIS DETECTION (TUNEL ANALYSIS)

Detection of apoptotic cells was performed coupling the terminal deoxnucleotidyl transferase-mediated dUTP nick-end labeling (TUNEL) assay and the cytological appearance of the cells. The TUNEL assay was performed according to the manufacturer's protocol (R&D systems, UK).

IMMUNOFLUORESCENCE STAINING

Sections were deparaffinized; pepsin digested as previously described[27] and blocked in serum free protein blocking solution (DAKO, UK). After overnight incubation with either rabbit antihuman/mouse Phospho-Histone H3 1:50 (PHH3; cell signaling technology, USA) or rabbit antihuman/mouse CP II antibodies 1:800 (kindly provided by Dr Lindsay King from IBEX, Canada), sections were incubated with cy™3 conjugated goat antirabbit antibody 1:600 (Jackson ImmunoResearch Laboratories, USA). Slides were mounted in Mowiol (Calbiochem, Merck Biosciences Ltd, Nottingham, UK) containing 4,6-diamindino-2-phenylindole (DAPI; ICN, Stretton Scientific Ltd, UK).

IMMUNOLOCALIZATION OF COLLAGENASE, AGGRECANASES AND MMPs INDUCED EPITOPES

Sections were deparaffinized and digested with chondroitinase ABC (Sigma, UK) in 0.1 M Tris–HCl, pH 8.0 for 1 h at 37°C. Endogenous peroxidase activity was quenched by incubating the sections with 3% H_2O_2. Sections were blocked and incubated overnight with the primary antibody: antiC1,2C (Col2-3/4Cshort) 1:800 (IBEX, Canada), anti-TEGE^{373} or anti-VDIPEN 1:10 (kindly provided by Professor Bruce Caterson and Dr Debbie Tudor, Cardiff University). Sections were incubated with EnVision®+Dual Link system-HRP (DakoCytomation, UK). DAB Substrate Chromogen System (DakoCytomation, UK) was used as peroxidase substrate. Sections were counterstained with hematoxylin and mounted with DPX (BDH, UK). The specificity of the stainings with positive and negative controls is shown in Supplementary Figure 1.

STATISTICAL ANALYSIS

The mean histological scores were compared using the Mann–Whitney *U* test for unpaired non-parametric data. Student's unpaired *t*-test was used for the other comparisons between the two strains. Differences were considered statistically significant when P was <0.05.

Results

REPRODUCIBILITY AND CONSISTENCY OF JOINT SURFACE INJURY

To assess the consistency of the experimental JSD at different levels within the same mouse, in different mice, and in mice of different strains, we compared histomorphometric measurements of cartilage thickness and injury size (Table II) at three different planes within the patellar groove of each mouse (Fig. 1B). The thickness of the articular cartilage within the analyzed interval was comparable in C57BL/6 and DBA/1 mice (Fig. 1C). Depth, CSW, and CSA of the defects were very consistent and highly reproducible within the same joint, and across different mice with no statistically significant difference between the two strains analyzed (Fig. 1C, D). Importantly, in all operated animals, the defects were consistently full thickness within the analyzed interval (Fig. 1E).

STRUCTURAL OUTCOME OF ACUTE JOINT SURFACE INJURY

One day after injury, there was no difference between the two adult strains as evaluated by histomorphometry (Fig. 1C–E) and histology (Fig. 2A). At 1-week time point, undifferentiated spindle shaped cells partially filled the defects in DBA/1 mice. By 4 weeks, the tissue filling the defects in DBA/1 mice consisted of chondrocytes surrounded by safranin-O stained matrix. However, this repair tissue lacked the typical architecture of normal articular cartilage as the superficial, intermediate, and deep layers were not morphologically distinguishable and the bone front had not reached the level of the osteochondral boundary as in the surrounding cartilage. After 8 weeks, there was a complete filling of the defects with well organized safranin-O positive hyaline-like cartilage (Fig. 2A). Polarized light microscopy showed fibers crossing the boundary between repair tissue and original cartilage, thereby indicating integration; however, superficial irregularities and fibrillar discontinuity were sometimes observed (not shown). In contrast, the lesions induced in C57BL/6 mice healed poorly as undifferentiated fibroblast-like cells invaded only the bottom of the defects 4 weeks after injury. At later time points, defects were partially filled with thin cancellous bone covered by a superficial layer of fibrous tissue (Fig. 2A). The repair scores in DBA/1 mice were statistically significantly lower (better repair) than C57BL/6 at 4 and 8 weeks after injury (Fig. 2C).

In addition to the different repair outcome, only C57BL/6 mice displayed progressive features of OA in the articular cartilage of the patellar groove as early as 1 week after injury. Initially, these features included small hypo- or a-cellular areas, surface fibrillation and faint safranin-O staining adjacent to the experimental defect. Subsequent, progression included cluster formation, clefts, focal lesions and loss of safranin-O metachromasia. Later on, these features extended to cartilage areas far from the experimental injury (Fig. 2A, B and D).

At all time points analyzed, no histological differences in the articular cartilage of the patellar groove were detected within the interval analyzed between the sham operated and non-operated controls from both strains as evaluated by H&E and safranin-O staining (Fig. 2A).

CELL DEATH AND PROLIFERATION

Apoptosis has been described as a pathogenic mechanism of cartilage breakdown in OA[28,29]. In the injured joints, apoptotic cells were identified in the proximity of the injury and at the edge of articular cartilage at day 1 in young mice of both strains (Fig. 3A, B). In consecutive H&E stained section, pyknotic nuclei were present in the same areas (Fig. 3C). In subsequent time points, chondrocyte apoptosis in DBA/1 mice progressively decreased and nearly disappeared at 4 and 8 weeks time points (Fig. 3A, B), whereas in C57BL/6 mice, after an initial flexion, apoptosis

Table II
The mean and the standard error of the mean (S.E.M.) of histomorphometric measurements

	Depth	CSW	CSA	% of Defect depth to cartilage thickness
C57BL/6	69.78 ± 4.33 μm, CV = 6.4%	149.55 ± 26.29 μm, CV = 19%	7302.4 ± 1258.05 μm^2, CV = 18.9%	106.37% ± 4.28
DBA/1	70.36 ± 3.84 μm, CV = 5.3%	141.31 ± 29.37 μm, CV = 22.3%	6988.2 ± 1541.56 μm^2, CV = 23.3%	104.64% ± 2.58

CV = coefficient of variation.

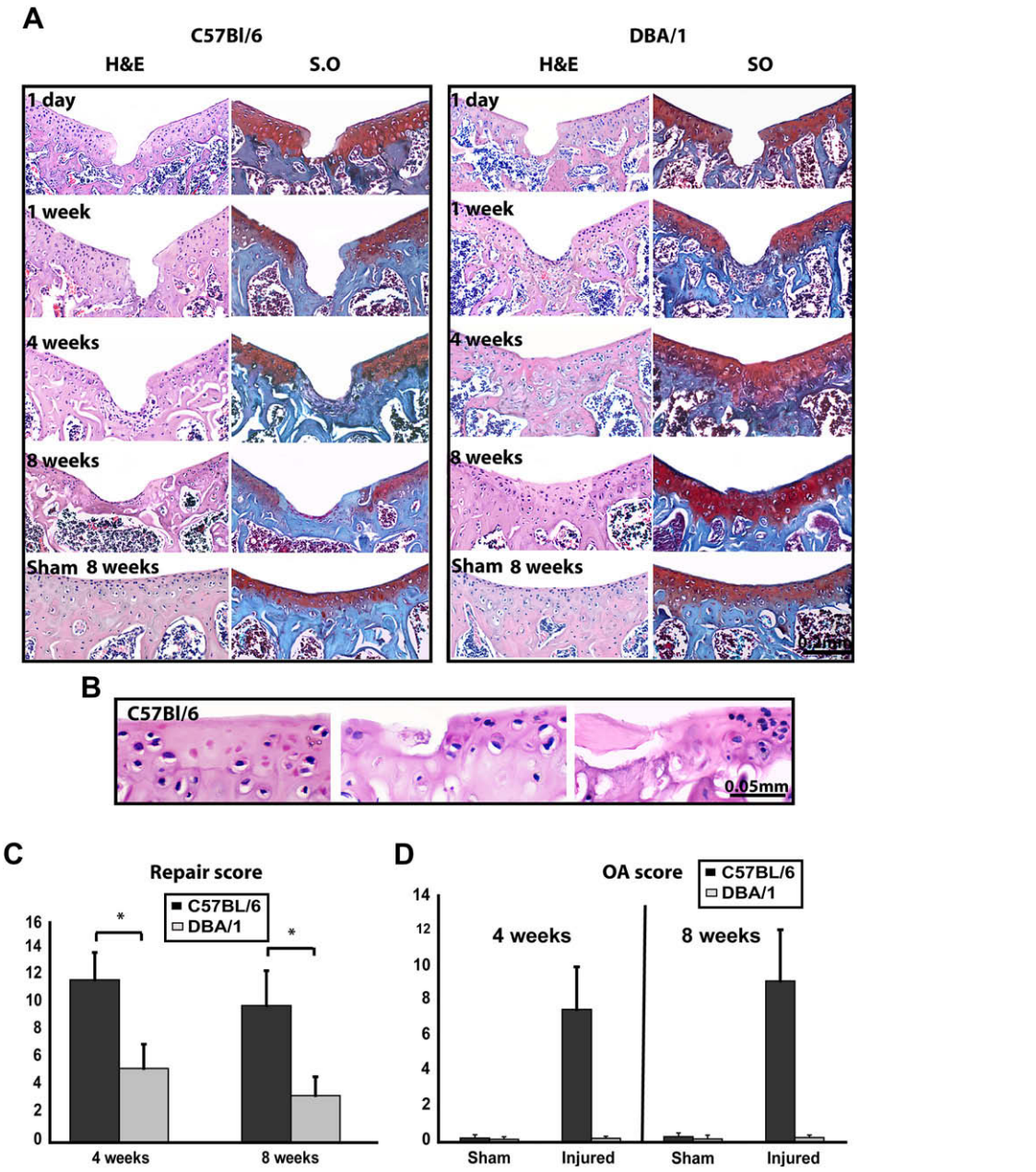

Fig. 2. Outcome of acute mechanical cartilage injury. (A) H&E (left) and safranin-O (right) staining of sections from sham operated and injured joints of 8 weeks old C57BL/6 and DBA/1 mice at the indicated time points. (B) Higher magnification of H&E stained sections from injured C57BL/6 showing areas away from the experimental lesion with various degrees of OA. (C−D), repair score (C) and modified Mankin score (D) at 4 ($n = 5$) and 8 ($n = 15$) weeks time points. Low score in C indicated better repair and high score in D indicated more severe OA. All the values are expressed as mean ± standard error of the mean (S.E.M.). $^*P < 0.05$. [For interpretation of color in this figure legend, the reader is referred to web version of the article.]

persisted, mainly around areas of cartilage degeneration, with statistically significant difference to DBA/1 mice (Fig. 3A−C). In the articular cartilage of the sham and non-operated knee joints, we did not detect any TUNEL-positive cells at all the time points analyzed (Fig. 3A).

Although chondrocyte proliferation has been reported to take place following injury[28], we only detected scattered proliferating cells within the repair tissue at 1 and 4 weeks following injury in DBA/1 mice but not in the articular cartilage adjacent to the injury in either of the two strains, as assessed by PHH3 staining (Fig. 3D).

TYPE II COLLAGEN NEO-SYNTHESIS AND DEGRADATION

To study type II collagen neo-synthesis, we immunostained the C-terminal telopeptide cleaved from type II procollagen molecules using antiCPII antibody[30]. In the control and sham-operated joints, the collagen C-telopeptide was detected in the mineralized deep layer of the articular cartilage (Fig. 4A). Following injury, pericellular CPII staining was observed in the superficial and intermediate zones. In these areas, collagen type II neo-synthesis peaked 1 week after injury in both strains, but subsequently declined

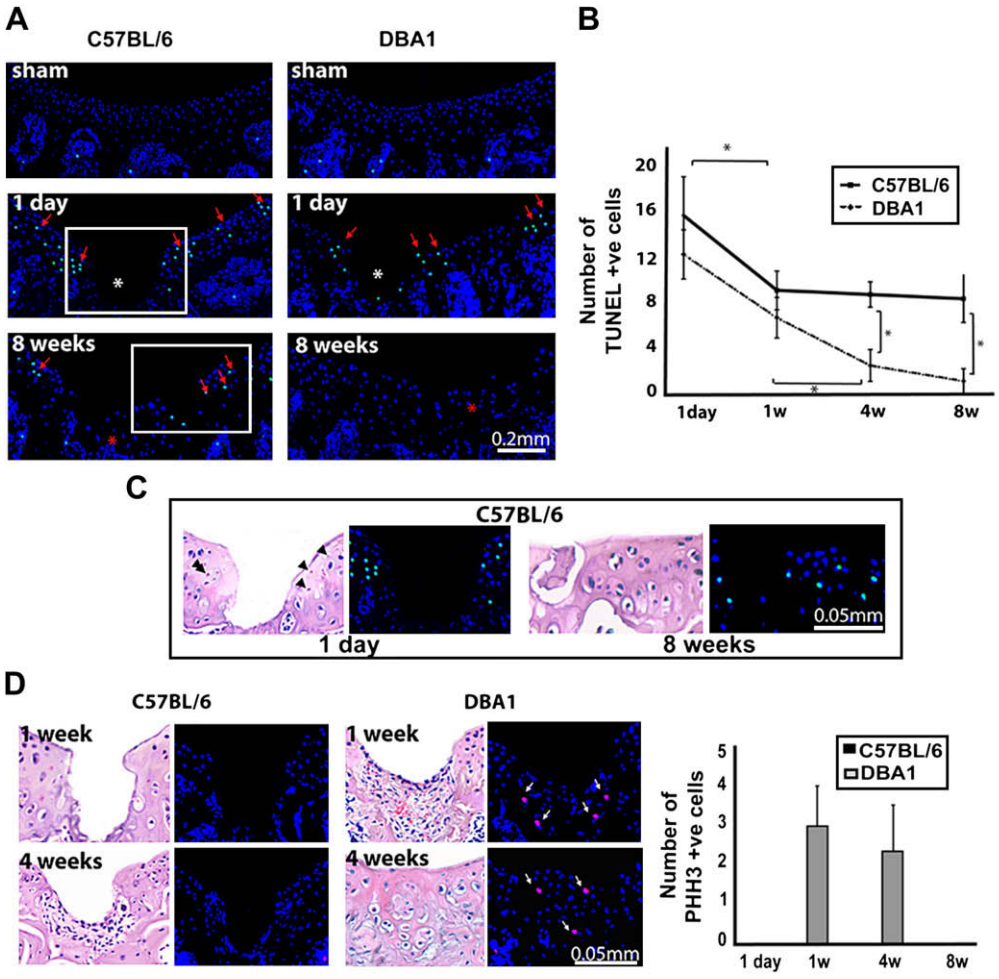

Fig. 3. Cell death and proliferation. (A), TUNEL assay in sham-operated and injured joints of young mice at 1 day and 8 weeks after injury. Red arrows indicate apoptotic nuclei (green). Nuclei are counterstained with DAPI (blue). The asterisk indicates the injury site. (B), Numbers of apoptotic cells at different time points comparing both strains. The values are expressed as mean and standard deviation of three different operated mice using three sections from each joint. $^{*}P < 0.05$. (C), Higher magnification of the areas squared in (A) at 1 day and 8 weeks time points, respectively, and H&E staining of a consecutive section. Pyknotic nuclei are indicated with black arrowheads. (D), Phospho-Histone H3 immunofluorescence, and H&E staining of a consecutive section at 1 and 4 weeks time points. White arrows indicate proliferating cells (red). Nuclei are counterstained with DAPI (blue). The numbers of proliferating cells counted in three mice using three sections from each joint are shown as mean and standard deviation. [For interpretation of color in this figure legend, the reader is referred to web version of the article.]

in C57BL/6, while persisted in DBA/1 mice for at least 8 weeks and became confined to the newly formed cartilage (Fig. 4A, B). The number of CPII-positive chondrocytes was statistically significantly higher in DBA/1 mice at 4 and 8 weeks time points (Fig. 4B).

We then compared type II collagen degradation in both strains utilizing anti C1, 2C (Col2-3/4C$_{short}$) antibody that recognizes the carboxy-terminal end of the collagenase-generated fragment of type II collagen. Intact uninjured articular cartilage from sham and non-operated joints showed weak pericellular C1, 2C staining in both C57BL/6 and DBA/1 young mice (Fig. 4C). As early as 1 week and for at least 8 weeks following injury, immunostaining increased in both strains. The repair tissue in DBA/1 mice, however, displayed a weaker staining than the adjacent cartilage (Fig. 4C).

AGGRECAN CLEAVAGE BY AGGRECANASES AND MMPs ACTIVITY

Proteoglycan turnover is central to cartilage homeostasis. To compare proteoglycan aggrecan breakdown in young mice from both strains *in vivo* following injury, we performed immunostaining for aggrecan neo-epitopes generated by aggrecanases and matrix metalloproteinases MMPs (TEGE^{373} and VDIPEN, respectively). In sham and non-operated control joints, both strains exhibited similar staining patterns (Fig. 5A, B). As early as 1 day after injury and thereafter, C57BL/6 mice displayed increased TEGE^{373} staining and low levels of VDIPEN. An opposite expression pattern was detected in DBA/1 mice with weak TEGE^{373} and intense VDIPEN staining (Fig. 5A, B). These findings indicate that aggrecan is prevalently degraded by aggrecanases in the C57BL/6 and by MMPs in DBA/1 strain.

THE REPAIR OUTCOME IN AGED MICE

Age is a factor influencing the outcome of JSD in humans[7,9] and animal models[31] with older individuals being less likely to have spontaneous healing. To investigate the effect of ageing, we challenged 8-month-old C57BL/6 and DBA/1 mice in this model. Aged animals from both strains reproducibly failed to repair the defect. However,

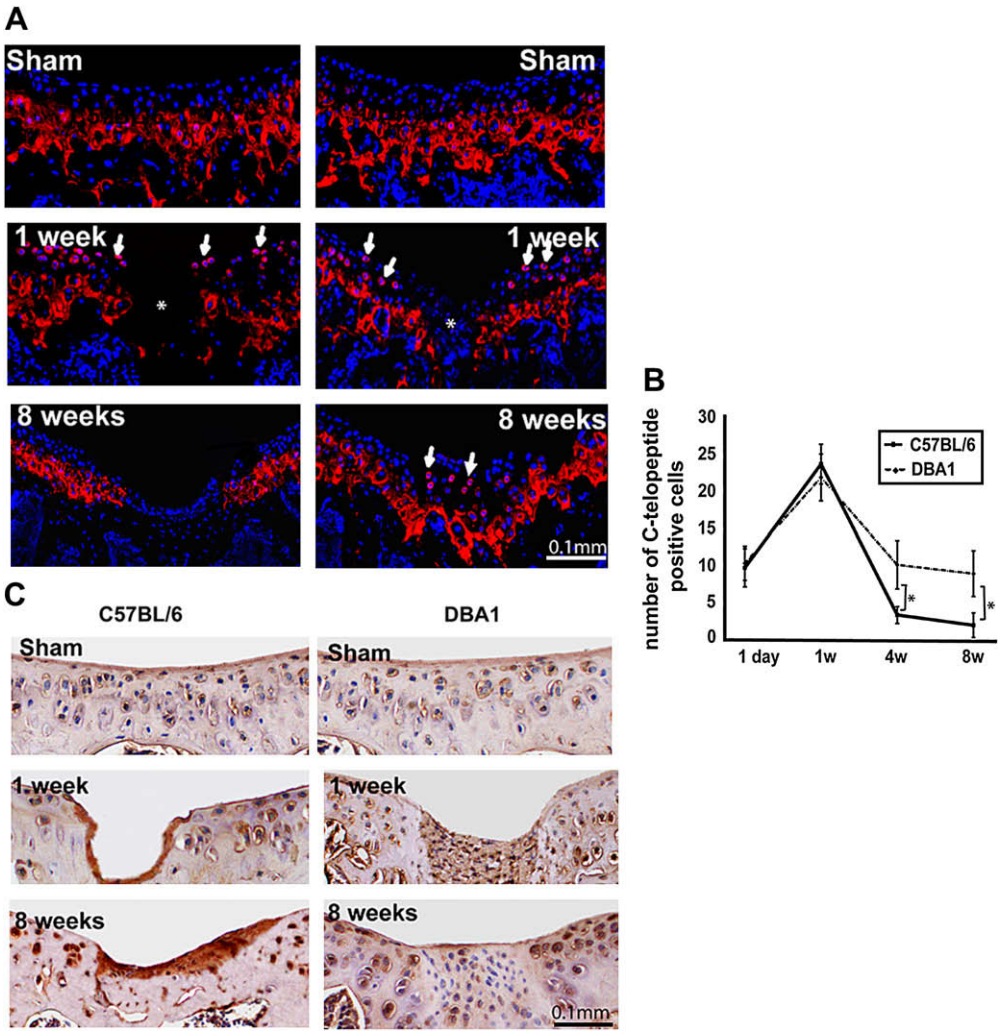

Fig. 4. Collagen synthesis and degradation. (A), Immunofluorescence staining for type II collagen C-telopeptide (A) in 8-week-old C57BL/6 (left) and DBA/1 (right). Type II collagen C-telopeptide is shown in red and nuclei are counterstained with DAPI (blue). (B), The number of C-telopeptide positive chondrocytes within the superficial and intermediate layer. The values from three different mice from each strains at the indicated time point are expressed as mean and standard deviation. $*P < 0.05$. (C), Immunostaining of C1, 2C neoepitope in C57BL/6 (left) and DBA/1 (right). Negligible staining is seen in the repair tissue in DBA/1 mice. [For interpretation of color in this figure legend, the reader is referred to web version of the article.]

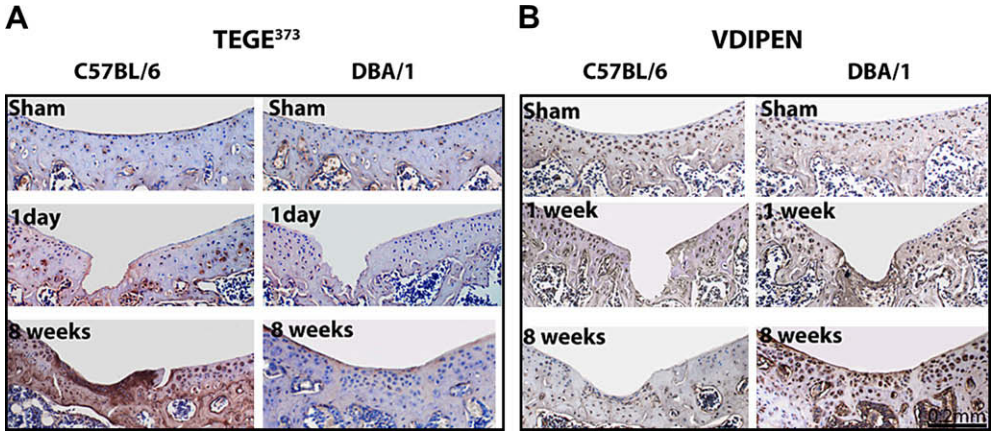

Fig. 5. Aggrecan degradation. Immunostaining of aggrecanase ($TEGE^{373}$, A) and MMPs (VDIPEN, B) generated neoepitope (brown) in the articular cartilage of 8-week-old C57BL/6 and DBA/1. Nuclei are counterstained with hematoxylin (blue). [For interpretation of color in this figure legend, the reader is referred to web version of the article.]

whereas C57BL/6 mice developed severe diffuse knee OA, DBA/1 mice did not show any sign of OA at all time points analyzed (Fig. 6).

Discussion

Traumatic cartilage lesions represent a common symptomatic and disabling problem[1,2] that often requires surgical intervention to relieve pain and to prevent possible evolution towards secondary OA[3,19,20]. The absence of relevant preclinical animal models of joint surface regeneration suitable for molecular studies and genetic manipulation has represented a bottleneck for the development of novel therapeutics to enhance/support joint surface repair. In this study, we have developed and characterized a mouse model of acute full thickness JSD with a strain and age dependent repair outcome. Adult DBA/1 mice reproducibly healed experimental joint surface lesions, whereas age-matched C57BL/6 healed poorly and instead developed features of secondary OA. Aged mice failed to repair, but, in contrast to age-matched C57BL/6 mice, DBA/1 developed no signs of secondary OA. The strain-dependent different outcome in young animals was associated with different regulation of apoptosis, proliferation and matrix remodeling.

Since the repair of JSD depends largely on their size and depth[7,9,10], the reproducibility of the injury in our model was an important concern. We therefore measured the size of the defects focusing the analysis on the interval between planes A and C (Fig. 1B) because, within this region, the articular cartilage is of uniform thickness and it is well exposed during surgery after patellar dislocation. Importantly, the intersection of the growth plate within these planes provided a useful anatomical landmark. We achieved a high reproducibility and consistency of the injury by combining a well controlled sampling technique within a selected anatomical area and the design of a simple and reliable device to induce the injury. Importantly, all the defects were full thickness in all the animals and slightly deeper than 100% of the cartilage thickness. Such consistency was largely ensured by the resistance offered by the subchondral bone, the resilience of the 26 G needle used to make the device, and the presence of the glass bead which by adapting to the concavity of the patellar groove, allowed the tip of the needle to run reproducibly in the centre of the patellar groove.

C57BL/6 mice develop spontaneous OA with ageing[32] and they are more susceptible than DBA/1 to OA induced by destabilization of the medial meniscus (DMM)[33]. However, spontaneous OA appears in C57BL/6 mice only after their first year of age, and no signs of OA were present in control or sham-operated joints in our study. It is therefore unlikely that pre-existing OA or joint instability inadvertently induced during surgery were the causes for repair failure. On the other hand, the generation of a JSD in C57BL/6 mice precipitated the appearance of secondary OA features as early as 1 week after injury. At 4 weeks, when the OA features in C57BL/6 mice had advanced, there was also a clear difference in repair outcome compared to DBA/1. It is possible that the rapid development of secondary OA may have conditioned repair failure. Our experimental setup does not discriminate whether the failure of repair and the development of OA are causally related, or if they represent distinct processes resulting from an inferior joint homeostatic mechanism in C57BL/6 than in DBA/1 mice. However, the observation that aged DBA/1 mice did not repair and did not develop OA either, under our experimental conditions and at the time points examined, demonstrates that repair failure alone may not be sufficient for the development of secondary OA and suggests that the two processes may be, at least in part, uncoupled.

On the other hand, DBA/1 mice are responsive to inflammatory arthritis models such as type II collagen-induced arthritis whereas C57BL/6 mice are resistant[34]. A modest infiltrate was present in the synovial membrane of the two strains during the first week following surgery (data not shown); however, it is possible that a different inflammatory response may play a role in repair outcomes.

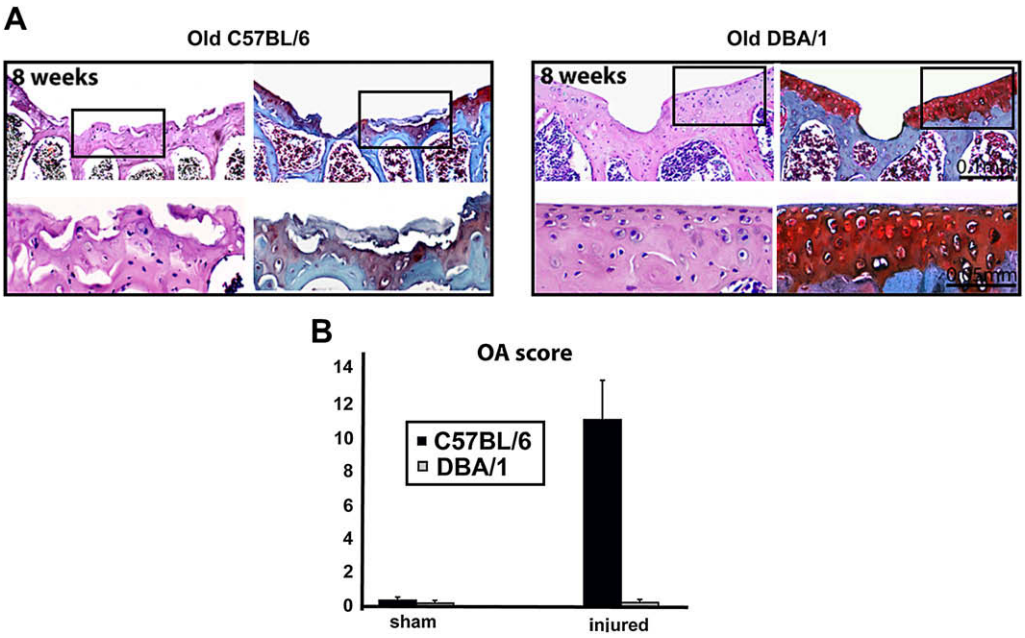

Fig. 6. Structural outcome in aged mice. (A), H&E (left) and safranin-O (right) staining of sections from injured joints of 8-month-old C57BL/6 and DBA/1 mice 8 weeks after surgery. The lower panel shows higher magnification of the areas squared in the upper panel. (B), Modified Mankin score at 8 weeks time points ($n = 15$). All the values are expressed as mean ± standard error of the mean (S.E.M.).

Non-differentiated spindle-like cells filled the lesions in DBA/1 mice at 1 week. In C57BL/6, morphologically similar cells appeared in the defects after 4 weeks when chondrogenesis had already occurred in DBA/1 mice. This delay in populating the wound could be due to differences reported in proliferation rate, cell surface epitopes and differentiation potential between bone marrow mesenchymal stem cells (MSCs) isolated from C57BL/6 and DBA/1 with higher chondrogenic potential of DBA/1 MSCs[35]. Additional potential mechanism could be a delayed activation/migration of mesenchymal progenitors in response to cartilage signals released by injured cartilage[27]. We recently showed that genes encoding morphogens, chemokines and other signaling molecules are activated in human adult articular cartilage after mechanical injury[36]. Failure of either the cartilage to deploy such response to injury or the mesenchymal progenitor/stem cells to respond to such signaling molecules may contribute to the delay of C57BL/6 mesenchymal cells in filling the defect.

Chondrocyte apoptosis progressively resolved in DBA/1 mice and persisted in C57BL/6 for at least 8 weeks. Chondrocyte death following mechanical injury and its potential role in the pathogenesis of OA have been described in several studies[28,29,37,38]. However, apoptotic cells may play a positive role in the repair responses by releasing chemo-attractants for stem/progenitor cells such as high mobility group box 1 (HMGB1)[39]. Therefore, it is possible that controlled chondrocyte apoptosis, in the initial phases of repair, may play a similar function after cartilage injury; however, it could be detrimental if not tightly regulated and inappropriately prolonged. Our experimental setup does not allow discriminating whether the prolonged apoptosis in C57BL/6 is determining or a consequence of repair failure.

Proliferation in the cartilage surrounding the injury site has been reported following mechanical trauma[28,40]. We did not detect chondrocyte proliferation in the articular cartilage surrounding the injury. However, proliferating cells were identified within the repair tissue in DBA/1 mice at 1 and 4 weeks post-surgery. This discrepancy with previous literature could be due to differences in the experimental conditions, the time points analyzed and the detection systems used. We examined the phosphorylation of histone H3 which is tightly correlated with the chromosome condensation phase during mitosis, thereby representing a snapshot of cells in M phase of cell cycle[41]. Conversely, incorporation of labeled nucleosides marks all the cells undergoing DNA duplication during the labeling period. Furthermore, cell proliferation in adult tissues occurs at a very low rate, and may take place in a short time-span after repair, thus our time points might have missed proliferation within the cartilage surrounding the injury. Surrounding tissues such as bone marrow and synovium have been proposed to contribute cells to the reparative process in different *in vivo* injury models[13,42]. However, the origin of the cells populating the defects and ultimately forming the repair cartilage in DBA/1 mice remains to be clarified.

Our study shows a prompt activation of matrix remodeling after injury within the repair tissue in DBA/1 mice and in the remaining cartilage in both strains. Matrix remodeling has been described in response to injury[28,43], during OA[44,45] and in human repair cartilage tissue obtained from ACI[46]. Interestingly, in this study, DBA/1 mice maintained a high level of collagen type II neo-synthesis and a low collagen catabolic activity for 8 weeks after injury. However, C57BL/6 mice exhibited a reverse pattern with progressive decrease in the number of CP II positive cells and intense Col2-3/4C$_{short}$ staining. Aggrecan degradation was prevalently driven by aggrecanases in C5BL/6 mice and by MMPs in DBA/1 mice.

Recently, ADAMTS-5 has been identified as the main aggrecanase in mouse cartilage and its ablation protected the mice from OA induced by DMM[47]. Similarly, mutants harboring a genetic allele of the aggrecan gene that blocks aggrecanases mediated cleavage were also protected when challenged in DMM model, but, interestingly, mice harboring an aggrecan mutant allele that is resistant to MMP-mediated cleavage developed more severe OA than their wild-type littermates[48]. Moreover, MMP9-deficient mice were more susceptible to OA than their wild-type littermates in the same model[33]. Taken together, these data and our results confirm the critical role of aggrecanases in cartilage destruction and suggest that a controlled level of MMP-mediated aggrecanolysis may be needed for cartilage homeostasis, and possibly repair, as MMPs proteolysis can facilitate cell migration, regulate tissue architecture, release and activate ECM bound growth factors and signaling molecules[49]. A caveat, in the interpretation of our data, is that aggrecan cleaved by aggrecanases may be internalized[50] and thereby no longer available for MMPs cleavage even in the presence of active MMPs. This may explain why, in C57BL/6, although several MMPs can cleave collagen and aggrecan, we only detected cleaved type II collagen. Another explanation for this discrepancy is that different MMPs may be responsible for aggrecan and collagen type II cleavage. Understanding these events would be crucial for the identification of the correct window of therapeutic intervention with inhibitors of aggrecanases and MMPs that are being developed and tested in preclinical and clinical studies[51].

The JSD repair encompasses highly coordinated biological events that require a fine tuning of diverse processes including cellular apoptosis, proliferation and tissue patterning regulated in a temporal–spatial manner. The molecular mechanisms regulating this process are poorly understood and their study has been hampered by the lack of suitable models. We anticipate that this new model of joint surface injury and repair, combined with mouse genetics, will be instrumental to elucidate the molecular control of these events, thereby enabling the development of new therapeutic agents to improve joint surface healing. It must stressed that this model is not a model of primary OA, but rather a model of joint surface injury and repair. However, the occurrence of post-traumatic OA features in C57BL/6 mice suggest it could be used to study the mechanism by which repair influences progression of post-traumatic secondary OA.

We and others[27,36,52,53] have demonstrated that the injured articular cartilage deploys a robust response to injury with activation of genes encoding signaling molecules and morphogens. This could be the effect of a putative repair response, or an adaptive response to damage, or could even play a role in post-traumatic secondary OA development. This model will allow addressing the functionality and hierarchy of molecules in the response to injury and subsequently represents a preclinical *in vivo* model to develop novel molecular therapeutics to support joint surface healing in cell-free *in situ* tissue engineering approaches.

Conflict of interest

We declare no conflict of interest in relation with this paper.

Acknowledgment

We would like to thank Professor Bruce Caterson and Dr Debbie Tudor, Cardiff University for kindly providing

anti-TEGE^{373} and anti-VDIPEN antibodies; Dr Lindsay King from IBEX, Canada for kindly providing the CP II antibody. We are grateful to the Arthritis Research Campaign (grant 16290) for funding this work, the UK Medical Research Council (grant G108/620) for supporting Professor De Bari's work, and the Egyptian government for funding Dr Eltawil PhD studentship (grant MM45/05).
This work has been funded by the UK Arthritis Research Campaign grant ID 16290, the UK Medical Research Council grant G108/620 and The Egyptian Government grant MM45/05.

Supplementary data

Supplementary data associated with this article can be found, in the online version, at doi:10.1016/j.joca.2008.11.003.

References

1. Curl WW, Krome J, Gordon ES, Rushing J, Smith BP, Poehling GG. Cartilage injuries: a review of 31,516 knee arthroscopies. Arthroscopy 1997;13:456–60.
2. Hjelle K, Solheim E, Strand T, Muri R, Brittberg M. Articular cartilage defects in 1,000 knee arthroscopies. Arthroscopy 2002;18:730–4.
3. Brittberg M, Peterson L, Sjogren-Jansson E, Tallheden T, Lindahl A. Articular cartilage engineering with autologous chondrocyte transplantation. A review of recent developments. J Bone Joint Surg Am 2003; 85-A(Suppl 3):109–15.
4. Ding C, Cicuttini F, Jones G. Tibial subchondral bone size and knee cartilage defects: relevance to knee osteoarthritis. Osteoarthritis Cartilage 2007;15:479–86.
5. Wluka AE, Ding C, Jones G, Cicuttini FM. The clinical correlates of articular cartilage defects in symptomatic knee osteoarthritis: a prospective study. Rheumatology (Oxford) 2005;44:1311–6.
6. Buckwalter JA, Brown TD. Joint injury, repair, and remodeling: roles in post-traumatic osteoarthritis. Clin Orthop Relat Res 2004;7–16.
7. Ding C, Cicuttini F, Scott F, Cooley H, Boon C, Jones G. Natural history of knee cartilage defects and factors affecting change. Arch Intern Med 2006;166:651–8.
8. vies-Tuck ML, Wluka AE, Wang Y, Teichtahl AJ, Jones G, Ding C, *et al*. The natural history of cartilage defects in people with knee osteoarthritis. Osteoarthritis Cartilage 2008;16:337–42.
9. Wang Y, Ding C, Wluka AE, Davis S, Ebeling PR, Jones G, *et al*. Factors affecting progression of knee cartilage defects in normal subjects over 2 years. Rheumatology (Oxford) 2006;45:79–84.
10. Buckwalter JA. Articular cartilage injuries. Clin Orthop Relat Res 2002; 21–37.
11. Messner K, Maletius W. The long-term prognosis for severe damage to weight-bearing cartilage in the knee: a 14-year clinical and radiographic follow-up in 28 young athletes. Acta Orthop Scand 1996;67: 165–8.
12. Shelbourne KD, Jari S, Gray T. Outcome of untreated traumatic articular cartilage defects of the knee: a natural history study. J Bone Joint Surg Am 2003;85-A(Suppl 2):8–16.
13. Shapiro F, Koide S, Glimcher MJ. Cell origin and differentiation in the repair of full-thickness defects of articular cartilage. J Bone Joint Surg Am 1993;75:532–53.
14. Breinan HA, Hsu HP, Spector M. Chondral defects in animal models: effects of selected repair procedures in canines. Clin Orthop Relat Res 2001;S219–30.
15. Convery FR, Akeson WH, Keown GH. The repair of large osteochondral defects. An experimental study in horses. Clin Orthop Relat Res 1972; 82:253–62.
16. De BC, Dell'accio F, Tylzanowski P, Luyten FP. . Multipotent mesenchymal stem cells from adult human synovial membrane. Arthritis Rheum 2001;44:1928–42.
17. Dowthwaite GP, Bishop JC, Redman SN, Khan IM, Rooney P, Evans DJ, *et al*. The surface of articular cartilage contains a progenitor cell population. J Cell Sci 2004;117:889–97.
18. De BC, Dell'accio F. Mesenchymal stem cells in rheumatology: a regenerative approach to joint repair. Clin Sci (Lond) 2007;113:339–48.
19. Beris AE, Lykissas MG, Papageorgiou CD, Georgoulis AD. Advances in articular cartilage repair. Injury 2005;36(Suppl 4):S14–23.
20. Smith GD, Knutsen G, Richardson JB. A clinical review of cartilage repair techniques. J Bone Joint Surg Br 2005;87:445–9.
21. De BC, Pitzalis C, Dell'accio F. Reparative medicine: from tissue engineering to joint surface regeneration. Regen Med 2006;1:59–69.
22. Steinert AF, Ghivizzani SC, Rethwilm A, Tuan RS, Evans CH, Noth U. Major biological obstacles for persistent cell-based regeneration of articular cartilage. Arthritis Res Ther 2007;9:213.
23. Wakitani S, Goto T, Pineda SJ, Young RG, Mansour JM, Caplan AI, *et al*. Mesenchymal cell-based repair of large, full-thickness defects of articular cartilage. J Bone Joint Surg Am 1994;76:579–92.
24. Koga H, Muneta T, Ju YJ, Nagase T, Nimura A, Mochizuki T, *et al*. Synovial stem cells are regionally specified according to local micro environments after implantation for cartilage regeneration. Stem Cells 2006.
25. Mankin HJ, Dorfman H, Lippiello L, Zarins A. Biochemical and metabolic abnormalities in articular cartilage from osteo-arthritic human hips. II. Correlation of morphology with biochemical and metabolic data. J Bone Joint Surg Am 1971;53:523–37.
26. van der Sluijs JA, Geesink RG, van der Linden AJ, Bulstra SK, Kuyer R, Drukker J. The reliability of the Mankin score for osteoarthritis. J Orthop Res 1992;10:58–61.
27. Dell'accio F, De BC, El Tawil NM, Barone F, Mitsiadis TA, O'Dowd J, *et al*. Activation of WNT and BMP signaling in adult human articular cartilage following mechanical injury. Arthritis Res Ther 2006;8:R139.
28. Redman SN, Dowthwaite GP, Thomson BM, Archer CW. The cellular responses of articular cartilage to sharp and blunt trauma. Osteoarthritis Cartilage 2004;12:106–16.
29. Tew SR, Kwan AP, Hann A, Thomson BM, Archer CW. The reactions of articular cartilage to experimental wounding: role of apoptosis. Arthritis Rheum 2000;43:215–25.
30. Lee ER, Smith CE, Poole R. Ultrastructural localization of the C-propeptide released from type II procollagen in fetal bovine growth plate cartilage. J Histochem Cytochem 1996;44:433–43.
31. Wei X, Gao J, Messner K. Maturation-dependent repair of untreated osteochondral defects in the rabbit knee joint. J Biomed Mater Res 1997; 34:63–72.
32. Wilhelmi G, Faust R. Suitability of the C57 black mouse as an experimental animal for the study of skeletal changes due to ageing, with special reference to osteo-arthrosis and its response to tribenoside. Pharmacology 1976;14:289–96.
33. Glasson SS. *In vivo* osteoarthritis target validation utilizing genetically-modified mice. Curr Drug Targets 2007;8:367–76.
34. Wooley PH, Luthra HS, Stuart JM, David CS. Type II collagen-induced arthritis in mice. I. Major histocompatibility complex (I region) linkage and antibody correlates. J Exp Med 1981;154:688–700.
35. Peister A, Mellad JA, Larson BL, Hall BM, Gibson LF, Prockop DJ. Adult stem cells from bone marrow (MSCs) isolated from different strains of inbred mice vary in surface epitopes, rates of proliferation, and differentiation potential. Blood 2004;103:1662–8.
36. Dell'accio F, De BC, Eltawil NM, Vanhummelen P, Pitzalis C. Identification of the molecular response of articular cartilage to injury, by microarray screening: Wnt-16 expression and signaling after injury and in osteoarthritis. Arthritis Rheum 2008;58:1410–21.
37. Hembree WC, Ward BD, Furman BD, Zura RD, Nichols LA, Guilak F, *et al*. Viability and apoptosis of human chondrocytes in osteochondral fragments following joint trauma. J Bone Joint Surg Br 2007;89: 1388–95.
38. Mistry D, Oue Y, Chambers MG, Kayser MV, Mason RM. Chondrocyte death during murine osteoarthritis. Osteoarthritis Cartilage 2004;12: 131–41.
39. Palumbo R, Galvez BG, Pusterla T, De MF, Cossu G, Marcu KB, *et al*. Cells migrating to sites of tissue damage in response to the danger signal HMGB1 require NF-kappaB activation. J Cell Biol 2007;179: 33–40.
40. Wong BJ, Pandhoh N, Truong MT, Diaz S, Chao K, Hou S, *et al*. Identification of chondrocyte proliferation following laser irradiation, thermal injury, and mechanical trauma. Lasers Surg Med 2005;37: 89–96.
41. Nowak SJ, Corces VG. Phosphorylation of histone H3: a balancing act between chromosome condensation and transcriptional activation. Trends Genet 2004;20:214–20.
42. Hunziker EB, Rosenberg LC. Repair of partial-thickness defects in articular cartilage: cell recruitment from the synovial membrane. J Bone Joint Surg Am 1996;78:721–33.
43. Aurich M, Mwale F, Reiner A, Mollenhauer JA, Anders JO, Fuhrmann RA, *et al*. Collagen and proteoglycan turnover in focally damaged human ankle cartilage: evidence for a generalized response and active matrix remodeling across the entire joint surface. Arthritis Rheum 2006;54:244–52.
44. Nelson F, Dahlberg L, Laverty S, Reiner A, Pidoux I, Ionescu M, *et al*. Evidence for altered synthesis of type II collagen in patients with osteoarthritis. J Clin Invest 1998;102:2115–25.
45. Bay-Jensen AC, Andersen TL, Charni-Ben TN, Kristensen PW, Kjaersgaard-Andersen P, Sandell L, *et al*. Biochemical markers of type II collagen breakdown and synthesis are positioned at specific sites in human osteoarthritic knee cartilage. Osteoarthritis Cartilage 2008;16:615–23.

46. Roberts S, Hollander AP, Caterson B, Menage J, Richardson JB. Matrix turnover in human cartilage repair tissue in autologous chondrocyte implantation. Arthritis Rheum 2001;44:2586–98.
47. Glasson SS, Askew R, Sheppard B, Carito B, Blanchet T, Ma HL, *et al*. Deletion of active ADAMTS5 prevents cartilage degradation in a murine model of osteoarthritis. Nature 2005;434:644–8.
48. Little CB, Meeker CT, Golub SB, Lawlor KE, Farmer PJ, Smith SM, *et al*. Blocking aggrecanase cleavage in the aggrecan interglobular domain abrogates cartilage erosion and promotes cartilage repair. J Clin Invest 2007;117:1627–36.
49. Page-McCaw A, Ewald AJ, Werb Z. Matrix metalloproteinases and the regulation of tissue remodelling. Nat Rev Mol Cell Biol 2007;8: 221–33.
50. Embry Flory JJ, Fosang AJ, Knudson W. The accumulation of intracellular ITEGE and DIPEN neoepitopes in bovine articular chondrocytes is mediated by CD44 internalization of hyaluronan. Arthritis Rheum 2006;54:443–54.
51. Murphy G, Nagase H. Reappraising metalloproteinases in rheumatoid arthritis and osteoarthritis: destruction or repair? Nat Clin Pract Rheumatol 2008.
52. Gruber J, Vincent TL, Hermansson M, Bolton M, Wait R, Saklatvala J. Induction of interleukin-1 in articular cartilage by explantation and cutting. Arthritis Rheum 2004;50:2539–46.
53. Vincent T, Hermansson M, Bolton M, Wait R, Saklatvala J. Basic FGF mediates an immediate response of articular cartilage to mechanical injury. Proc Natl Acad Sci U S A 2002;99:8259–64.